Environ. Res. Lett. **4** (2009) 044013 (9pp) doi:10.1088/1748-9326/4/4/044013

# Deactivation of ice nuclei due to atmospherically relevant surface coatings

**Daniel J Cziczo[1,2,7], Karl D Froyd[3,4], Stephane J Gallavardin[1,5], Ottmar Moehler[6], Stefan Benz[6], Harald Saathoff[6] and Daniel M Murphy[3]**

[1] Institute for Atmospheric and Climate Science, ETH Zurich, Universitätstrasse 16, CH-8092, Zürich, Switzerland
[2] Atmospheric Science and Global Change Division, Pacific Northwest National Laboratory, 902 Battelle Boulevard, Richland, WA 99354, USA
[3] Chemical Sciences Division, National Oceanic and Atmospheric Administration, 325 Broadway Avenue, Boulder, CO 80305, USA
[4] Cooperative Institute for Research in Environmental Sciences, University of Colorado, 216 UCB, Boulder, CO 80309, USA
[5] Institute for Atmospheric Physics, Johannes Gutenberg University Mainz, D-55128, Mainz, Germany
[6] Institute for Meteorology and Climate Research, Karlsruhe Institute of Technology, Postfach 3640, D-76021, Karlsruhe, Germany

E-mail: daniel.cziczo@pnl.gov

Received 4 September 2009
Accepted for publication 12 November 2009
Published 23 November 2009
Online at stacks.iop.org/ERL/4/044013

**Abstract**
The ice nucleation characteristics of Arizona test dust (ATD) and illite clay, surrogates for atmospheric ice nuclei, have been determined at the Aerosol Interactions and Dynamics in the Atmosphere (AIDA) chamber located at the Research Center Karlsruhe in Germany. The objective of this research was to determine the effect of sulfuric acid and ammonium sulfate coatings on the ability of these mineral dust surrogates to nucleate ice in an environment where particles realistically compete for water vapor. Coated ATD particles required higher saturations at all temperatures considered, from −20 to −45 °C, than did identical uncoated particles. Freezing of coated particles often required saturations approaching those for the homogeneous freezing of aqueous solutions of the coating material alone. Less pronounced effects were found for illite, although the presence of a coating consistently increased the saturation or decreased the temperature required for ice formation. Analysis of ice residue at the single particle level suggests that the first coated particles to freeze had thinner or incomplete coatings when compared to particles that froze later in the expansion. This observation highlights a need to verify coating properties since an assumption of homogeneity of a group of coated aerosols may be incorrect. The increase in saturation ratio for freezing suggests that gas-phase uptake of sulfates, a large fraction of which are due to anthropogenic emissions, will reduce the ice and mixed-phase cloud formation potential of atmospheric ice nuclei.

**Keywords:** ice nucleation, mineral dust, sulfuric acid, ammonium sulfate, cloud chamber

[7] Author to whom any correspondence should be addressed.

 

## 1. Introduction

Atmospheric ice formation takes place via two distinct pathways. The majority of atmospheric particles throughout the depth of the troposphere are aqueous mixtures of sulfates, organics and nitrates, neutralized to some extent by ammonia (Murphy and Thomson 1997, Murphy *et al* 2006). These aqueous particles require temperatures below approximately −38 °C and saturations near that of liquid water before the spontaneous formation of ice occurs (Koop *et al* 2000). This process is termed homogeneous freezing. Freezing which occurs above this temperature or below this saturation requires the presence of a special ice nucleus (IN) that stabilizes the formation of a water ice embryo (Pruppacher and Klett 1997). This process is termed heterogeneous freezing and it can occur via several distinct sub-pathways. These include the deposition of ice on a surface, freezing within a condensation layer, or by an IN fully immersed in a droplet (Pruppacher and Klett 1997). Less well studied to date is the process of freezing when an IN contacts a droplet (Cantrell and Heymsfield 2005).

The formation of ice in cirrus and mixed-phase clouds is among the most uncertain aspects of global climate change (IPCC 2007). This lack of certainty highlights a need for more comprehensive studies of the conditions at which IN initiate freezing. It is known from laboratory and field studies that mineral dust aerosols are among the most atmospherically common and effective IN (i.e., they require the highest temperature and lowest saturation; Pruppacher and Klett 1997). Other particles, for example carbonaceous cores from biomass burning and fossil fuel combustion, are more atmospherically common (Murphy *et al* 2006) but less effective as IN (DeMott *et al* 2003a, Dymarska *et al* 2006). A few bacteria and some other bioaerosols such as pollen have been shown to be effective IN (Möhler *et al* 2007, Pratt *et al* 2009) but their atmospheric abundance and distribution are not known and appears to be extremely low. For example bacterial mass spectrometric patterns have been resolved (Fergenson *et al* 2004) but they have not been found in great numbers during atmospheric studies.

Given their combined large atmospheric burden (Usher *et al* 2003) and ice formation potential (Pruppacher and Klett 1997, DeMott *et al* 2003b), mineral dusts are of considerable interest in cloud formation, precipitation initiation, and the global radiative balance. Gas-phase components such as nitrates, sulfates, and organics are known to adhere to mineral dust surfaces (Murphy and Thomson 1997, Grassian 2002). The effect of these surface layers is to increase the ability of the normally insoluble and hydrophobic mineral dust core to take up water and form cloud droplets (Levin *et al* 1996, Herich *et al* 2009). The theoretical effect of the formation of coatings due to the uptake of gas-phase species on ice nucleation as well as due to coagulation with pre-existing particles is summarized by Pruppacher and Klett (1997): whereas the coating process enhances cloud drop formation it has been suggested to 'deactivate' ice nucleation.

More recently, sulfate coating experiments have been conducted by Zuberi *et al* (2002) who studied kaolinite and montmorillonite and Hung *et al* (2003) who studied hematite and corundum mineral dust cores immersed within larger ammonium sulfate droplets using optical microscopy and infrared spectroscopy, respectively. Ettner *et al* (2004) also optically studied freezing of multiple kaolinite and montmorillonite inclusions in large sulfuric acid droplets (>1 mm diameter) levitated by acoustic forces. Zobrist *et al* (2008) used differential scanning calorimetry and optical techniques to observe several possible IN, including silica and ATD, within several inorganic salts and organics including ammonium sulfate and sulfuric acid. Due to instrumental limitations the majority of these studies were on super-micrometer droplets and were only able to compare the required freezing conditions to pure droplets of the coating material, not to uncoated mineral dust (i.e., immersion versus homogeneous freezing only). In all cases the presence of an immersed nucleus initiated freezing at higher temperatures than required for homogeneous freezing of the coating material alone.

Organic coating experiments have been undertaken by Kanji *et al* (2008) who compared ice nucleation of silica with silica coated with an octyl chain in a thermal gradient chamber. Möhler *et al* (2008) undertook experiments in the AIDA chamber with organic coatings from the reaction of ozone with $\alpha$-pinene on mineral dust cores of ATD and the clay illite. Both research groups concluded that organics 'deactivated' the IN, resulting in a higher saturation and/or a lower required temperature for ice formation. Möhler *et al* (2008) also found that homogeneous freezing of the pure organic was, in all cases, less effective than material with an immersed dust particle.

Eastwood *et al* (2009) investigated the clay kaolinite both in a bare state and coated with sulfuric acid and ammonium sulfate. Eastwood *et al* (2009) also found that aqueous coatings in all cases inhibited ice nucleation although crystalline ammonium sulfate had little or no effect on the IN. Archuleta *et al* (2005) performed experiments in a continuous flow diffusion chamber on variable-sized metal oxides and alumina silicates from 50 to 200 nm diameter both in an uncoated state and coated with sulfate. Archuleta *et al* found that the effect of the coating depended on the core material. Specifically, sulfate appeared to enhance ice nucleation in about 50% of the studied samples of iron oxide whereas the alumina silicates were predominantly deactivated by a coating. Aluminum oxide was not affected. The coated and uncoated mineral dust particles were in all cases more effective at ice formation than the homogeneous freezing of the coating material alone. Knopf and Koop (2006) investigated bare ATD and particles coated with sulfuric acid. In agreement with the finding of Archuleta *et al* (2005) for aluminum oxide, but contrary to the findings of Eastwood *et al* (2009), Knopf and Koop (2006) found little or no coating effect on IN potential. Specific experimental conditions are compared in section 4.

In this study we have undertaken freezing experiments on ATD and illite clay, meant to be representative of atmospheric mineral dust particles. We have determined the saturation required, as a function of temperature, for ice nucleation by uncoated as well as particles coated with sulfuric acid or ammonium sulfate. These results are compared to the

**Table 1.** Coating and aerosol properties. ATD and illite particles were uncoated or coated with sulfuric acid (SA) or ammonium sulfate (AS). A higher saturation temperature ($T_{SA,sat}$) in the coating unit resulted in a thicker coating. Also given are the initial gas temperature $T_{g,0}$ and aerosol number concentration $n_{ae,0}$ in the AIDA chamber measured just before the start of the expansion.

| Expansion | Coating | $T_{SA,sat}$ (°C) | $T_{g,0}$ (°C) | $n_{ae,0}$ (cm$^{-3}$) | Notes |
|---|---|---|---|---|---|
| 1 | ATD uncoated | — | −30.2 | 234 | |
| 2 | ATD uncoated | — | −30.2 | 153 | |
| 3 | ATD uncoated | — | −30.3 | 98 | |
| 8 | ATD SA | 130 | −32.3 | 184 | |
| 9 | ATD SA | 130 | −31 | 120 | |
| 10 | ATD AS | 130 | −30.8 | 75 | |
| 17 | ATD SA | 130 | −43.9 | 156 | |
| 18 | ATD AS | 130 | −45.1 | 109 | |
| 23 | ATD uncoated | — | −19.5 | 300 | |
| 24 | ATD uncoated | — | −19.4 | 211 | |
| 26 | ATD SA | 120 | −19.3 | 309 | Little freezing |
| 27 | ATD SA | 120 | −19.2 | 181 | Little freezing |
| 28 | ATD AS | 120 | −19.3 | 95 | Little freezing |
| 11 | Illite uncoated | — | −30.6 | 255 | |
| 12 | Illite uncoated | — | −30.5 | 185 | |
| 13 | Illite uncoated | — | −30.4 | 122 | |
| 14 | Illite SA | | −30.4 | 267 | |
| 15 | Illite SA | | −30.4 | 188 | |
| 16 | Illite AS | | −30.5 | 133 | |

homogeneous freezing threshold of the pure coating material. Both coated and uncoated ATD are more effective at ice formation than the homogeneous freezing of the pure coating material. Bare ATD is more effective than coated ATD from −20 to −45 °C, the range of temperatures investigated in this study. The deposition, immersion, and contact freezing modes that are possible in the atmosphere are all also possible in the cloud chamber.

## 2. Experimental methods

Experiments were conducted during fall 2005 as part of the IN08 campaign at the AIDA cloud chamber located at the Karlsruhe Institute of Technology in Germany. AIDA is an 84 m$^3$ actively cooled aluminum chamber with a diameter of 4 m. The chamber is evacuated before experiments to a pressure <0.1 hPa and is then refilled with particle-free air (background density <0.1 cm$^{-3}$). Particles of a known composition and size can then be added to the chamber. For the ice nucleation experiments described here the chamber was set to a constant temperature between −20 and −30 °C. Mixing with a fan was used to keep the temperature variability within the chamber below ±0.3 °C. The pre-experimental pressure was, for these studies, ∼1000 hPa. Humidity conditions were near the saturation pressure of ice at the wall temperature and were set by a thin coating of ice on the inner surface of the chamber.

Ice nucleation was initiated by inducing an expansion within the chamber with vacuum pumping. While the chamber walls remained at an essentially constant temperature the pressure within the vessel was dropped by ∼200 hPa over the course of a few minutes. This can be visualized in figure 1(a) where the gas pressure during a typical expansion, in this case the 17th of the campaign which utilized ATD coated with sulfuric acid at −45 °C, is plotted. The result is a corresponding drop in the gas temperature and increase in the relative humidity (panel (b)). This pressure drop rate mimics the process of uplift in the atmosphere, corresponding to a velocity of ∼0.1–2 m s$^{-1}$. A description of aerosol properties is given in table 1 and expansion conditions in table 2.

**Table 2.** Experimental conditions. The ice nucleation onset temperature $T_{0.01}$, relative humidity with respect to ice $RH_{i0.01}$, and relative humidity with respect to water $RH_{w0.01}$ correspond to an ice-active aerosol particle number fraction of 1%. The mode of ice nucleation is indicated in the last column. During experiments 26, 27, and 28, only a few ice particles formed at about −26 °C with a number fraction below 0.01. The freezing modes were derived from the $RH_w$ and Welas measurements. When $RH_w$ remained below 100% and there was no indication of the formation of droplets deposition nucleation is noted. In experiments with $RH_w$ at 100% where the formation of ice was only observed after droplets had formed immersion freezing is noted. Formation of ice observed with $RH_w$ close to 100% is noted as either deposition or condensation/immersion freezing.

| Expansion | $T_{0.01}$ (°C) | $RH_{i0.01}$ (%) | $RH_{w0.01}$ (%) | Mode |
|---|---|---|---|---|
| 1 | −33 | 102 | 73 | Deposition |
| 2 | −33 | 108 | 80 | Deposition |
| 3 | −34 | 120 | 87 | Deposition |
| 8 | −36.4 | 136 | 96 | Immersion |
| 9 | −34.8 | 134 | 96 | Immersion |
| 10 | −34.8 | 136 | 97 | Immersion |
| 17 | −48.5 | 138 | 86 | Immersion, some deposition |
| 18 | −50.7 | 148 | 92 | Immersion, some deposition |
| 23 | −22.5 | 122 | 98 | Condensation |
| 24 | −22.5 | 122 | 98 | Condensation |
| 26 | — | — | — | Few IN at −26 °C |
| 27 | — | — | — | Few IN at −26 °C |
| 28 | — | — | — | Few IN at −26 °C |
| 11 | −34.4 | 127 | 91 | Deposition |
| 12 | −34.6 | 129 | 92 | Deposition |
| 13 | −34.8 | 130 | 93 | Deposition |
| 14 | −35.0 | 128 | 91 | Deposition/immersion |
| 15 | −36.5 | 129 | 91 | Deposition/immersion |
| 16 | −37.7 | 127 | 88 | Deposition (Immersion?) |

As the relative humidity increased and the temperature decreased, ice nucleation was initiated by some fraction of the aerosol in the chamber. This can be visualized in figure 1(c) where the number fraction $f_{ice} = n_{ice}/n_{ae}$ of particles which nucleated ice is plotted (right axis). The total aerosol number concentration $n_{ae}$ is also plotted in this panel (left axis). In addition to the formation of new ice, post-nucleation crystals deplete water vapor via growth (panel (d)). The initiation of ice formation by a given fraction of the aerosol (i.e., their cloud formation potential) can thus be related to a temperature and relative humidity using data of the type shown in figure 1. Ice nucleation continued until the combination of the expansion ending and ice crystal sedimentation depleted the gas-phase water until it ultimately relaxed to an equilibrium with the ice on the chamber walls. These measurements require the concerted effort of several independent instruments including facility temperature, pressure and a tunable diode laser for water vapor pressure measurements. A comprehensive list of these instruments and a schematic of the AIDA chamber

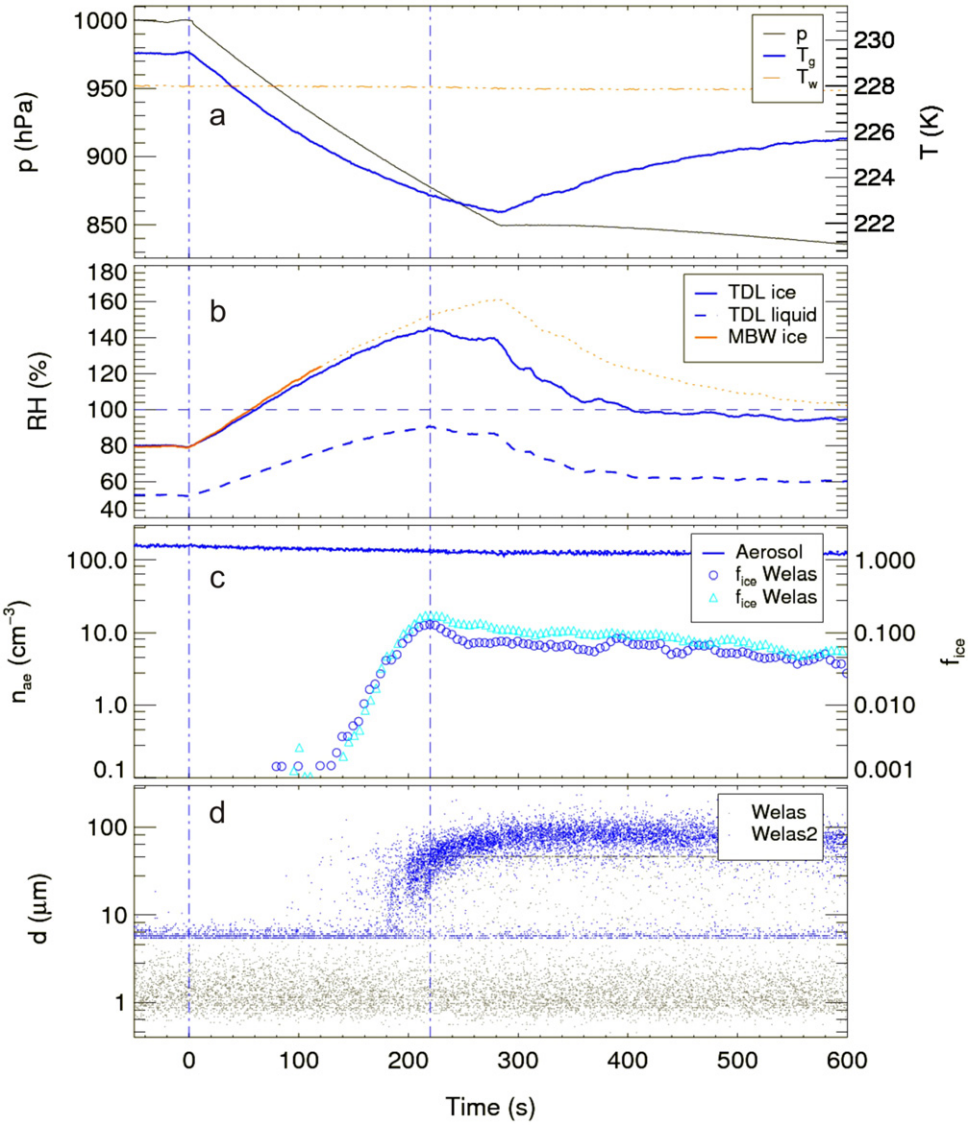


**Figure 1.** A typical AIDA expansion. This expansion, IN08-17 (i.e., the 17th expansion of the fall 2005 campaign), resulted in immersion and some deposition freezing. This expansion was conducted on sulfuric acid coated ATD at −45 °C. Panel (a) is the response of the gas-phase pressure to vacuum pumping with respect to time and the corresponding gas and wall temperature profiles. Panel (b) relates the effect on the relative humidity with respect to ice (i.e., $RH_i$) and liquid water (i.e., $RH_w$; Murphy and Koop 2005) using a tunable diode laser and MBW frost point hygrometer. Panel (c) is the concentration of aerosol and of ice crystals formed as discerned by a CPC and the Welas and Welas2 instruments, respectively. Panel (d) shows the evolution of crystal growth. Note that Welas2 overestimates ice crystal sizes for $d > 30$ $\mu$m. See text for further details.

is given in Möhler *et al* (2008). A condensation particle counter (CPC; TSI Inc. model CPC3010) for aerosol number density and two optical particle counters (Palas GmbH, Welas type) for ice crystal concentration were also connected to the chamber via sampling tubes. The two versions of the Welas type OPC, located within the cold section surrounding the AIDA chamber, were used with different size ranges and sensitivities for single particle detection. Assuming spherical particles with a refractive index of 1.33, Welas and Welas2 detect particles with diameters from 0.8 $\mu$m to 46 $\mu$m and from 9.0 $\mu$m to 237 $\mu$m, respectively. For non-spherical ice particles, both instruments are only used in the counting mode to measure ice particle concentrations. No attempt was made to quantitatively derive crystal sizes from the Welas scatter intensities. Nevertheless, growing ice particles can be detected and distinguished from large aerosol particles or droplets of almost constant size during the AIDA expansion experiments. For concentration measurements of 1.0 $cm^{-3}$ for Welas and 0.3 $cm^{-3}$ for Welas2 the counting uncertainty was less than ±50% (i.e., more than 4 counts) for acquisition periods of 10 s.

Aerosol particles were generated from samples which were used and characterized in earlier studies (Möhler *et al* 2006, 2008). Dry samples were first aerosolized with a rotating brush disperser (RBG-1000, Palas) and then further deagglomerated in a dispersion nozzle. The resulting aerosol was passed through a cyclone impactor to remove particles larger than ∼1 $\mu$m in diameter and was then added to the aerosol preparation and characterization (APC) chamber, a

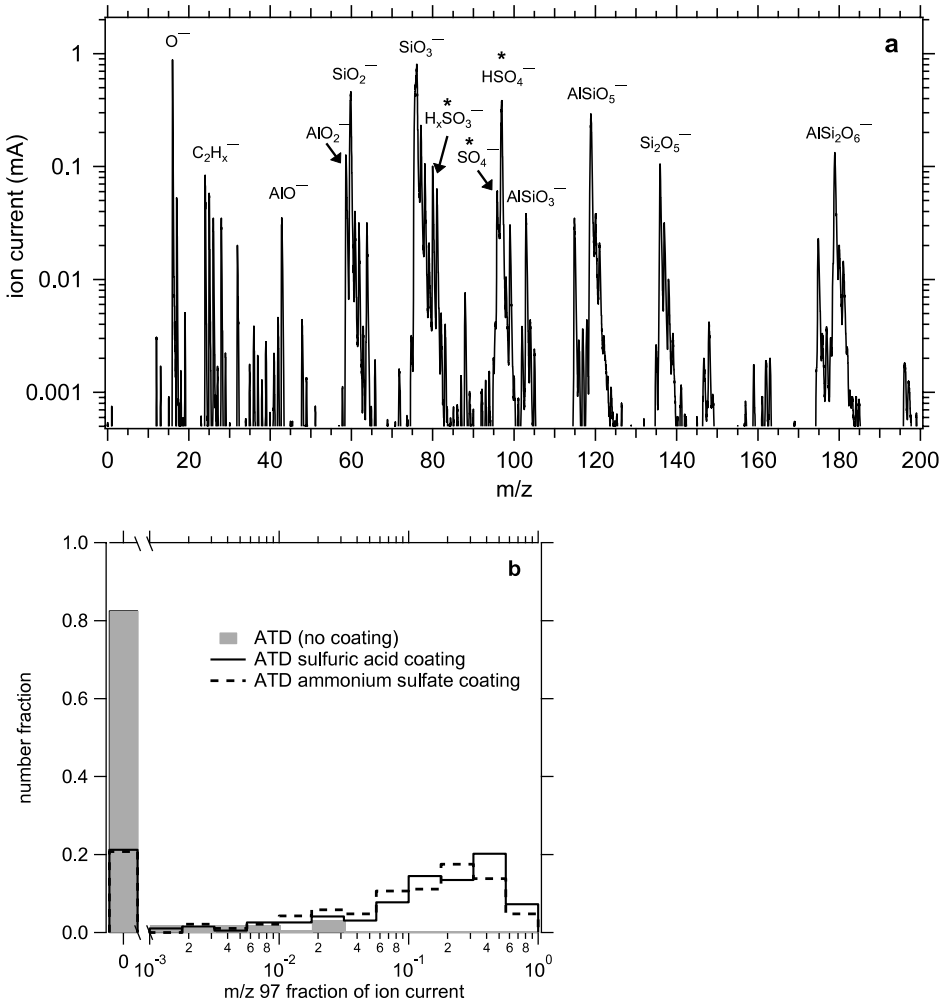


**Figure 2.** Coating signatures. Panel (a) is a negative polarity mass spectrum of ATD with sulfate coating where * denotes coating signatures. Note that negative polarity ammonium sulfate coating signatures are identical ions. Panel (b) is a histogram of primary sulfate signal intensity for uncoated and coated ATD. Most spectra with $m/z$ 97 intensity >0.01 represent coated ATD. About 20% of ATD particles that underwent the coating process did not show a coating signature. See text for further details.

3.7 $m^3$ volume outside AIDA, and uniformly distributed with the help of a mixing fan. Both the brush disperser and the dispersion nozzle were operated with dry and particle-free synthetic air to avoid contamination of the dust aerosol with particles of unknown origin. From the APC chamber a minor fraction of the dust aerosol was passed through a stainless steel connection tube to the large AIDA cloud chamber. Particles were coated with $H_2SO_4$ when the flow from the aerosol generator was mixed at a temperature of ∼150 °C with a flow of synthetic air saturated with sulfuric acid vapor. The sulfuric acid condensed to the dust particles upon slow cooling of the mixture. The coating amount was varied by selecting different sulfuric acid saturation temperatures of the synthetic air flow (see table 1). Ion chromatography of bulk filter samples collected during the experiments showed average sulfuric acid concentration of ∼10% by mass and with a range from 5 to 20%. The coated dust aerosol was also added to the APC chamber and from there transferred into the larger AIDA cloud chamber. Coating with ammonium sulfate was achieved inside the AIDA chamber. Ammonia gas was added to the chamber in excess to the amount of sulfuric acid. The particles took up ammonia until the sulfuric acid layers were fully neutralized to ammonium sulfate. Fourier transform infrared spectroscopy was used to verify composition.

Single particle mass spectrometry was performed on the test aerosol before and after, and on the ice residue during, expansions. This technique was used to distinguish the presence or absence, and give a rough indication of the extent of surface coatings. Aerosol was directly removed from the APC chamber or AIDA before or after expansions. During expansions a pumped counterflow virtual impactor (PCVI) was used to inertially separate crystals from aerosol which did not form ice (Boulter *et al* 2006). The crystals were exposed to a warm and dry counterflow such that condensed-phase water was evaporated. The residual particles were then conducted to the particle analysis by laser mass spectrometry (PALMS) instrument. PALMS draws particles into the instrument and focuses them using an aerodynamic inlet and differential pumping stages. Particles are detected and aerodynamically sized as they scatter light from two visible 532 nm YAG lasers set 34 mm apart. Sizing is accomplished because particles exiting the aerodynamic lens are accelerated to a size-

dependent velocity and this is determined by recording the transit time between the visible lasers. A 193 nm excimer laser is then triggered to strike the particle, thereby ablating and ionizing the components. Positive or negative ions are then accelerated in a reflectron mass spectrometer flight tube and detected as a function of their mass. Particle size and monopolar chemical composition are thus recorded on the single particle level *in situ* and in real time. A comprehensive instrument description of PALMS is provided in Cziczo *et al* (2006) and the PCVI-PALMS combination has been utilized at the AIDA chamber previously (Gallavardin *et al* 2008). It is noteworthy that aerodynamic focusing and optical detection restrict the particle size range to 200–3000 nm, but within this range both refractory (e.g., mineral dust) and semi-volatile (e.g., sulfates and organics) components are resolved (figure 2). Although not inherently quantitative, single particle mass spectrometer trends in ion signal can be used as an indication of relative abundance (Murphy *et al* 2006, Spencer and Prather 2006). For ionizable substances particle fractions on the order of 1% (i.e., monolayer-level coatings) are detectable. Figure 2(a) is an exemplary negative polarity mass spectrum of a coated ATD particle to illustrate the ions associated with sulfate coatings. Panel (b) is a histogram which shows the distribution of the coating signal among particles in an experiment where all particles were subject to the aforementioned coating process (see section 3).

## 3. Results

Expansions were conducted to determine freezing onset temperature and saturation of uncoated and sulfuric acid and ammonium sulfate coated particles at approximately −20, −30 and −45 °C. The ice nucleation onsets in this work are defined as the threshold condition for an ice-active particle number fraction $f_{ice}$ of 1%, and were obtained from respective scatter plots of $f_{ice}$ versus the temperature and the relative humidity with respect to ice and to water. Results for the various expansions are plotted in figure 3. The homogeneous freezing line for 500 nm diameter particles is plotted for reference (Koop *et al* 2000). The most important result of this study is that atmospherically relevant coatings decrease the ice formation potential of very efficient ice nuclei. Specifically, coatings of sulfuric acid and ammonium sulfate increased the saturation and/or decreased the temperatures required for the formation of ice by ATD particles. In the extreme case of experiments at ∼−20 °C coated particles were not observed to freeze up to the saturation of liquid water whereas uncoated particles did freeze. At lower temperatures coated particles were observed to freeze but a higher saturation was required. At −50 °C, for example, freezing occurred at 30–40% higher $RH_i$ for coated ATD. Furthermore, sulfuric acid and ammonium sulfate coated ATD did not freeze until conditions were near the homogeneous freezing threshold. Particles coated with ammonium sulfate at all temperatures required slightly higher saturations for the onset of freezing (by a few $\%RH_i$) than sulfuric acid. The difference between uncoated and coated particles of both types was in all cases greater than the difference between the coatings.

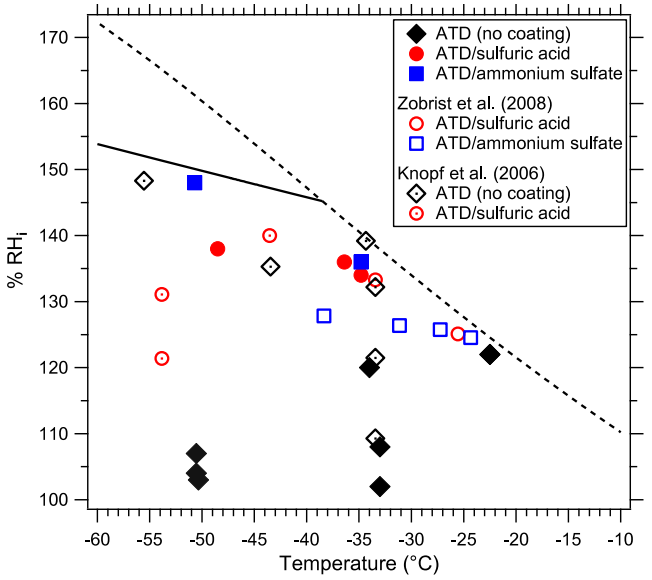


**Figure 3.** Ice nucleation onset conditions at the level of 1% of particles from this work for uncoated, sulfuric acid and ammonium sulfate coated ATD particles. Previous studies include uncoated and sulfuric acid coated ATD from Knopf and Koop (2006) for experiments where aerosols were not pre-activated, and sulfuric acid and ammonium sulfate coated ATD from Zobrist *et al* (2008). Water saturation (dashed) and homogeneous freezing curves for 500 nm particles at 1 $min^{-1}$ (solid) are shown for reference. ATD points at −51 °C are from Möhler *et al* (2006). See text for further details.

The sulfuric acid and ammonium sulfate coatings were detected by PALMS primarily as the presence of the $m/z$ 97 ($HSO_4^-$) ion (figure 2(a)). This peak was present for ∼80% of the coated particles larger than 200 nm. A distribution of coating signal was observed as shown in figure 2(b). PALMS does not ablate and ionize the entire particle for dust of the sizes used here. The absence of a sulfate peak is ambiguous as to whether that particle was completely uncoated or the PALMS ion signal came from a bare spot. In either case, the implications for heterogeneous ice nucleation are the same: there were uncoated portions of the particle available for nucleation.

Particles that nucleated relatively early in an expansion had different compositions than those that nucleated later. First, particles that nucleated early were those that had incomplete or thinner coatings than aerosols in the main freezing segment. Figure 4(a) shows the time series of the fraction of ice particle residues with a coating signature at $m/z$ 97 for IN08-17 (ATD coated with sulfuric acid). A lower fraction of the earliest nucleating aerosols had a coating signature, and average coating intensity was relatively low at <160 s. If single particle analysis is used to disregard this early nucleation segment when coating signal was absent or low, the freezing onset conditions for sulfuric acid coated ATD shift by as much as $25\%RH_i$ and −2.5 °C. Second, early nucleation of stainless steel contamination particles generated inside the chamber was occasionally observed, as in expansion IN08-18 (figure 4(b); ATD coated with ammonium sulfate). The residue composition began to reflect coated mineral dust at 25% higher $RH_i$ and 3.5 °C lower temperature than the initial freezing due to stainless steel.

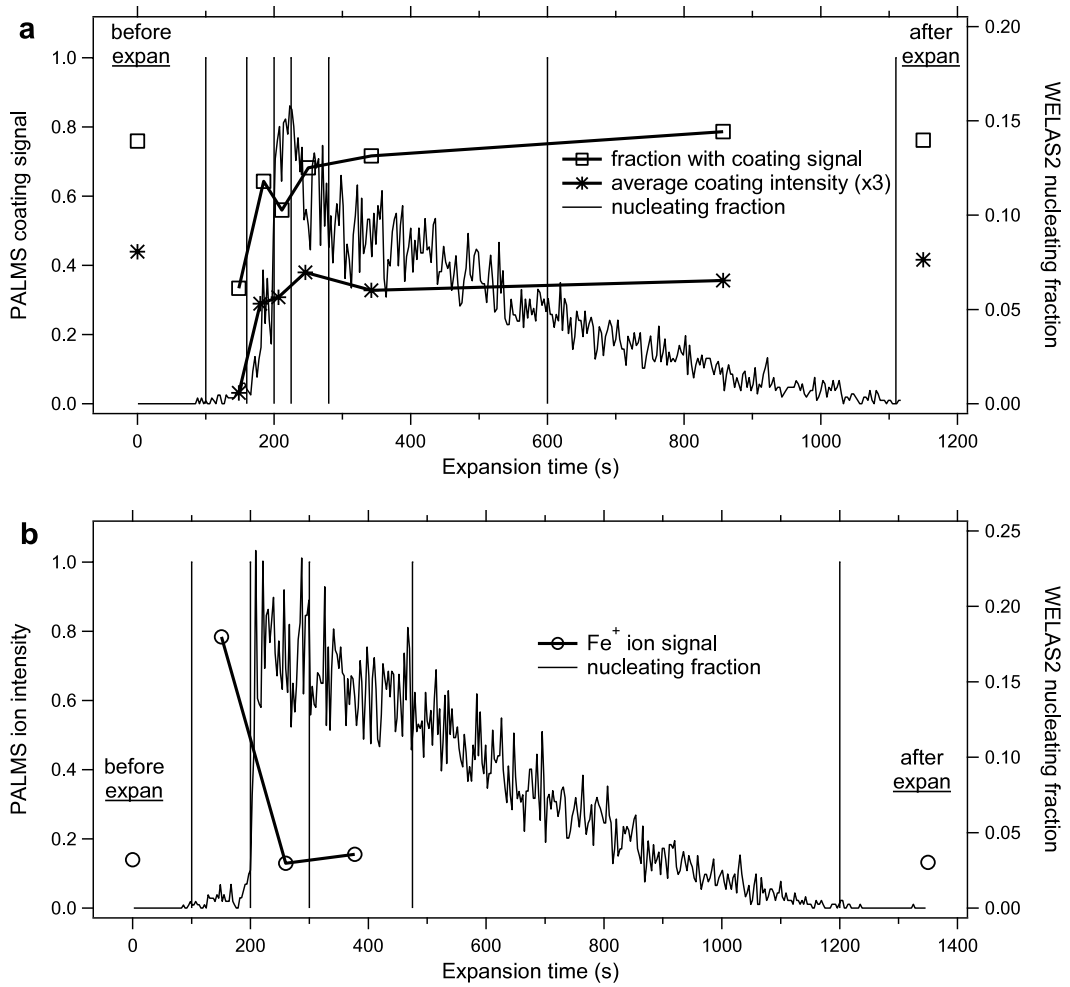


**Figure 4.** Trends in ion signal over the course of expansion. Panel (a) is for IN08-17, ATD with sulfuric acid coating at −45 °C. Fraction of residue spectra with a coating signal ($m/z$ 97 intensity >0.01; see figure 2) and average ion intensity of coating signals (scaled by a factor of 3 for clarity) are plotted. Averages are calculated before and after the expansion and for each time bin, represented by vertical lines. Note that particles which exhibit no or minimal coating are observed to be the first to nucleate ice (i.e., they are more effective IN). Panel (b) is for IN08-18, ATD with ammonium sulfate coating at −45 °C. Initial freezing in this expansion is by stainless steel contamination particles at <200 s as indicated by very high iron ion signals.

Expansions were also conducted on sulfuric acid and ammonium sulfate coated and uncoated illite particles at ∼−35 °C. Freezing of the uncoated aerosol was slightly lower (by a few %$RH_i$) than coated particles. The freezing point of the uncoated aerosol was considerable higher, ∼130%$RH_i$, than ATD (100–120%$RH_i$) at this temperature. This example shows that the characteristics of the nucleus (e.g., composition, surface morphology, etc) as well as the coating state of the aerosol are important determinates in freezing potential.

Mass spectral signals for refractory mineral dust components were also investigated. As in previous studies, ice residues were often enriched in lead (Cziczo *et al* 2009). Other than lead, a trace element found in mineral dust, little indication of preferential nucleation due to any major mineral component of ATD or illite was found. Occasionally, minor differences in nucleating behavior correlated with ion signals for lithium, barium, and strontium, but the effects were small and no clear trends could be identified. Condensation of gas-phase sulfuric acid, nitric acid, and organic species present in the background chamber air onto ice crystals was observed throughout these studies (Gallavardin *et al* 2008).

## 4. Discussion

The trend in ice nucleation behavior in this study is consistent with the results of Eastwood *et al* (2009) who found that the ice nucleation threshold of the clay kaolinite was increased from $RH_i$ ∼ 110% to ∼140% in the temperature range from −27 to −40 °C when coated with aqueous sulfuric acid and ammonium sulfate. In that study particles of ∼15 $\mu$m diameter were coated with ∼0.7 $\mu$m of sulfate. Möhler *et al* (2008) similarly found that organic coatings required an increase in $RH_i$ from 10 to 50% between −68 and −73 °C depending on thickness. In that study particles were of ATD and the clay illite from 100 nm to 1 $\mu$m diameter coated with from 17 to 41 wt% organic material. Archuleta *et al* (2005) found that the $RH_i$ required to nucleate 1% of alumina silicate particles, the major component of ATD, between 50 and 200 nm diameter was increased by ∼15%$RH_i$ between −45 and −60 °C. Coatings of 3–7 layers of sulfuric acid were used.

The results of Knopf and Koop (2006) are plotted with the data from this study in figure 3. Knopf and Koop (2006) found that ATD nucleated ice over a broad range, from ∼100 $RH_i$ to ∼100 $RH_w$ from −13 to −38 °C. From −38 to −78 °C ATD was observed to nucleate ice over the range from ∼100%$RH_i$ up to homogeneous freezing threshold. Particles from 700 nm to 10 $\mu$m diameter were investigated. Sulfuric acid coatings from 67 to 1100 layers were not observed to affect this range. Note, however, that this wide nucleation range precluded precise identification of difference in freezing behavior. Zobrist *et al* (2008) determined ice nucleation onset conditions for super-micrometer diameter particles, approximately an order of magnitude larger in diameter than those used in this study, coated with sulfuric acid and ammonium sulfate. These aerosols froze at a slightly lower humidity which is not surprising given their much greater surface. These data are also plotted in figure 3. Uncoated ATD was not investigated by Zobrist *et al* (2008) due to instrumental limitations.

Archuleta *et al* (2005) observed that aluminum oxide was unaffected by sulfuric acid coatings and that iron oxides were rendered slightly more effective, by ∼5%$RH_i$, ice nuclei. Coatings, temperatures, and particle sizes were the same as for the previously described experiments on alumina silicates. Our observations were that the effect of a coating was less pronounced on illite than on ATD. We did not observe cases where coatings enhanced or had no effect on ice nucleation as is given by Archuleta *et al* (2005). As a general conclusion, the nature of the ice nucleus and the coating, in addition to the particle size, are important determinates in the conditions required for freezing.

The use of single particle analysis in our study shows that the particle-to-particle variability in coating presence and thickness can have a large effect on the freezing point. Distributions of nominally 'coated' particles actually contained particles with no sulfate signal. Because in any given batch all particles were exposed to sulfuric acid vapor under the same conditions, the lack of a sulfate signal from some particles is somewhat difficult to understand. Electron microscopy of atmospheric mineral dust often shows that materials such as sulfates do not evenly coat a surface but are instead preferentially found in distinct locations (Buseck and Posfai 1999). Ice nucleation has been shown to occur at specific sites on the surface of mineral dust, often steps or other dislocations (Pruppacher and Klett 1997). This may also be true of the deposition of sulfates although a critical amount would ultimately surround the entire particle. In the case of deposition mode, and experiments below the deliquescence point of ammonium sulfates, this may help to explain the presence of bare mineral areas on which ice nucleated. In the case of studies in which droplet formation occurred (i.e., immersion and deposition mode) even an incomplete coating would be expected to activated and ultimately surround the dust particle with an aqueous solution. This suggests that the coating material was completely absent on some particles in these experiments.

The mass spectrometric observation of partially or fully uncoated particles is independently supported by the expansion experiments since those particles are also more effective ice nuclei than particles with large sulfate signals. We find here that up to a 25%$RH_i$ difference is apparent between particles with a small or no coating signal and those with a large signal. The heterogeneity of the coating is almost certainly related to the amount of coating material with monolayer coatings much more likely to be heterogeneous than those thicker than the diameter of the core particle. The occurrence of incomplete coatings in previous experiments, as well as the effect on results, is unknown because, to our knowledge, this is the first ice nucleation study that employed single particle mass spectrometry as an analytical technique.

The consensus of recent experiments is that coatings render bare mineral dust IN less effective or, at the least, have little effect. This is in agreement with theoretical arguments summarized by Pruppacher and Klett (1997). It has been shown that sulfate from anthropogenic sources can result in a coating on mineral dust (Kandler *et al* 2007). Increased emissions of sulfate by anthropogenic sources may therefore increase the coating on aerosol particles that otherwise may have either not been coated or coated to a lesser extent. This may then result in a deactivation of ice nuclei and an increase in the saturation required for cloud formation above pre-industrial levels. The effects of deactivation of dust by coatings is just beginning to be explored with global models (Hoose *et al* 2008) and, to our knowledge, is not included in current estimates of indirect aerosol forcing.

## Acknowledgments

We are grateful for the logistical and technical support provided by David Thomson and the AIDA staff. Funding was provided by ETH, NOAA, ACCENT, the European project SCOUT-O3 (GOCE-CT-2004-505390) and the PNNL Aerosol Initiative.

## References

Archuleta C M, DeMott P J and Kreidenweis S M 2005 Ice nucleation by surrogates for atmospheric mineral dust and mineral dust/sulphate particles at cirrus temperatures *Atmos. Chem. Phys.* **5** 2617–34

Boulter J E, Cziczo D J, Middlebrook A M, Thomson D S and Murphy D M 2006 Design and performance of a pumped counterflow virtual impactor *Aerosol Sci. Technol.* **40** 969–76

Buseck P R and Posfai M 1999 Airborne minerals and related aerosol particles: effects on climate and the environment *Proc. Natl Acad. Sci.* **96** 3372–9

Cantrell W and Heymsfield A 2005 Production of ice in tropospheric clouds *Bull. Am. Meteorol. Soc.* **86** 795–807

Cziczo D J, Thomson D S, Thompson T L, DeMott P D and Murphy D M 2006 Particle analysis by laser mass spectrometry (PALMS) studies of ice nuclei and other low number density particles *Int. J. Mass Spectrom.* **258** 21–9

Cziczo D J *et al* 2009 Inadvertent climate modification due to anthropogenic lead *Nat. Geosci.* **2** 333–6

DeMott P J, Cziczo D J, Prenni A J, Murphy D M, Kreidenweis S M, Thomson D S, Borys R and Rogers D C 2003a Measurements of the concentration and composition of nuclei for cirrus formation *Proc. Natl Acad. Sci.* **100** 14655–60

DeMott P J, Sassen K, Poellot M R, Baumgardner D, Rogers D C, Brooks S D, Prenni A J and Kreidenweis S M 2003b African dust aerosols as atmospheric ice nuclei *Geophys. Res. Lett.* **30** 1732

Dymarska M, Murray B J, Sun L M, Eastwood M L, Knopf D A and Bertram A K 2006 Deposition ice nucleation on soot at temperatures relevant for the lower troposphere *J. Geophys. Res. Atmos.* **111** D04204

Eastwood M L, Cremel S, Wheeler M, Murray B J, Girard E and Bertram A K 2009 Effects of sulphuric acid and ammonium sulphate coatings on the ice nucleation properties of kaolinite particles *Geophys. Res. Lett.* **36** L02811

Ettner M, Mitra S K and Borrmann S 2004 Heterogeneous freezing of single sulphuric acid solution droplets: laboratory experiments utilizing an acoustic levitator *Atmos. Chem. Phys.* **4** 1925–32

Fergenson D P *et al* 2004 Reagentless detection and classification of individual bioaerosols particles in seconds *Anal. Chem.* **76** 373–8

Gallavardin S J, Froyd K D, Lohmann U, Möhler O, Murphy D M and Cziczo D J 2008 Single particle laser mass spectrometry applied to differential ice nucleation experiments at the AIDA chamber *Aerosol Sci. Technol.* **42** 1–19

Grassian V 2002 Chemical reactions of nitrogen oxides on the surface of oxide, carbonate, soot, and mineral dust particles: implications for the chemical balance of the troposphere *J. Phys. Chem.* A **106** 860–77

Herich H, Tritscher T, Wiacek A, Gysel M, Weingartner E, Lohmann U, Baltensperger U and Cziczo D 2009 Water uptake of clay and desert dust aerosol particles at sub-and supersaturated water vapor conditions *Phys. Chem. Chem. Phys.* **11** 7804–9

Hoose C, Lohmann U, Erdin R and Tegen I 2008 The global influence of dust mineralogical composition on heterogeneous ice nucleation in mixed-phase clouds *Environ. Res. Lett.* **3** 025003

Hung H M, Malinowski A and Martin S T 2003 Kinetics of heterogeneous ice nucleation on the surfaces of mineral dust cores inserted into aqueous ammonium sulphate particles *J. Phys. Chem.* A **107** 1296–306

IPCC 2007 *Climate Change 2007: The Scientific Basis-Contributions of Working Group I to the Third Assessment Report of the Intergovernmental Panel on Climate Change*

Kandler K *et al* 2007 Chemical composition and complex refractive index of saharan mineral dust at izana tenerife (Spain) derived by electron microscopy *Atmos. Environ.* **41** 8058–74

Kanji Z A, Florea O and Abbatt J P D 2008 Ice formation via deposition nucleation on mineral dust and organics: dependence of onset relative humidity on total particulate surface areas *Environ. Res. Lett.* **3** 025004

Knopf D A and Koop T 2006 Heterogeneous nucleation of ice on surrogates of mineral dust *J. Geophys. Res.* **111** D12201

Koop T, Luo B P, Tsias A and Peter T 2000 Water activity as the determinant for homogeneous ice nucleation in aqueous solutions *Nature* **406** 611–4

Levin Z, Ganor E and Gladstein V 1996 The effects of desert particles coated with sulfate on rain formation in the Eastern Mediterranean *J. App. Met.* **35** 1511–23

Möhler O, Benz S, Saathoff H, Schnaiter M, Wagner R, Schneider J, Walter S, Ebert V and Wagner S 2008 The effect of organic coating on the heterogeneous ice nucleation efficiency of mineral dust aerosols *Environ. Res. Lett.* **3** 025007

Möhler O, DeMott P J and Levin Z 2007 Microbiology and atmospheric processes: the role of biological particles in cloud physics *Biogeosciences* **4** 1059–71

Möhler O *et al* 2006 Efficiency of the deposition mode ice nucleation on mineral dust particles *Atmos. Chem. Phys.* **6** 3007–21

Murphy D M, Cziczo D J, Froyd K D, Hudson P K, Matthew B M, Middlebrook A M, Peltier R E, Sullivan A, Thomson D S and Weber R J 2006 Single-particle mass spectrometry of tropospheric aerosol particles *J. Geophys. Res.* **111** D23S32

Murphy D M and Koop T 2005 Review of the vapour pressures of ice and supercooled water for atmospheric applications *Q. J. R. Meteorol. Soc.* **131** 1539–65

Murphy D M and Thomson D S 1997 Chemical composition of single aerosol particles at Idaho hill: negative ion measurements *J. Geophys. Res.* **102** 6353–68

Pratt K A *et al* 2009 *In situ* detection of biological particles in cloud ice-crystals *Nat. Geosci.* **2** 398–401

Pruppacher H R and Klett J D 1997 *Microphysics of Clouds and Precipitation* (Dordrecht: Kluwer)

Salam A, Lohmann U and Lesin G 2007 Ice nucleation of ammonia gas exposed montmorillonite mineral dust particles *Atmos. Chem. Phys.* **7** 3923–31

Spencer M T and Prather K A 2006 Using ATOFMS to determine OC/EC mass fractions in particles *Aerosol Sci. Technol.* **40** 585–94

Usher C R, Michel A E, Stec D and Grassian V H 2003 Laboratory studies of ozone uptake on processed mineral dust *Atmos. Environ.* **37** 5337–47

Zobrist B, Marcolli C, Peter T and Koop T 2008 Heterogeneous ice nucleation in aqueous solutions: the role of water activity *J. Phys. Chem.* A **112** 3965–75

Zuberi B, Bertram A K, Cassa C A, Molina L T and Molina M J 2002 Heterogeneous nucleation of ice in $(NH_4)_2SO_4$–$H_2O$ particles with mineral dust immersions *Geophys. Res. Lett.* **29** 1504